Localized Momentum-Space Distribution of Photocurrents Injected by Quantum Interference of Nonlinear Absorption Processes

Yiming Gong¹, Kai Wang², Steven T. Cundiff¹

¹ Department of Physics, University of Michigan, Ann Arbor, Michigan, 48109, USA ²School of Physics and Astronomy, Sun Yat-sen University, Zhuhai Campus, Zhuhai, Guangdong,519000, China

Abstract: Based on polarization dependence, we show that momentum-space distribution of photocurrents is more localized in quantum interference of two- and three-photon absorptions than that in quantum interference of one- and two-photon absorptions.

Optical absorption processes exciting the same carriers can interfere constructively in some regions of the Brillouin zone (BZ), and destructively in the opposite regions, resulting in a net injected current. As shown in Figure 1 (a) and (b), quantum interference control (QuIC) of carriers can be achieved in AlGaAs using one- and two-photon absorption (1+2 QuIC) [1] or two- and three-absorption (2+3 QuIC) [2]. The distribution of injected carriers has been predicted to be more localized in the azimuthal direction in 2+3 QuIC than that in 1+2 QuIC [3]. The increased localization can be beneficial to developing optical methods that are sensitive to band structure. To probe the k-space azimuthal distribution of injected carriers, we compared the direction in real space of injection photocurrents produced by 1+2 QuIC and 2+3 QuIC.

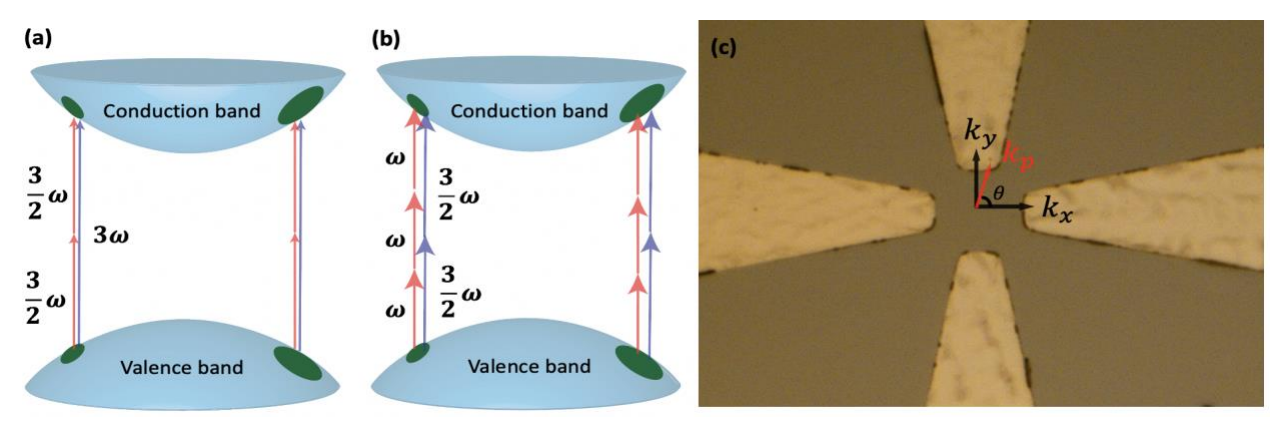


Figure 1: Depictions of (a) 1+2 QuIC and (b) 2+3 QuIC showing the destructive (left) and constructive (right) interference in different regions of the Brillouin zone. (c) Two pairs of electrodes detect photocurrents flowing in two perpendicular directions. k_x and k_y are aligned to [100] and [010] crystal axis. The polarizations of two excitation fields are along k_p .

As shown in Figure 1(c), four metallic electrodes were deposited on a AlGaAs wafer by optical lithography. The device was made from epitaxially grown AlGaAs on a GaAs substrate. Five layers of Au, Ge, and Ni were deposited and annealing at 450 C for 5 minutes was used to create ohmic contact with a metal-semiconductor-metal structure, where QuIC signal behaved as a current source. We used a custom fiber laser system (MenloSystems) producing a frequency comb with output at 1560 nm and 1040 nm derived from a common femtosecond oscillator with a repetition rate of 250.583 MHz. The 1560 nm and 1040 nm beams are respectively referred to as ω and $3\omega/2$ fields in Figure 1. 1+2 and 2+3 QuIC photocurrents were measured separately using two different experimental setups.

To observe 1+2 QuIC, 2ω was generated by frequency doubling of the 1040 nm frequency comb with a β -barium borate (BBO) crystal. The second harmonic and fundamental light were separated using a prism pair. The temporal delay between second harmonic and fundamental light was controlled by an optical delay line. The two beams were combined and focused on the center of four electrodes by a 60X objective. A piezo attached to the optical delay line was dithered the relative phase at 2 kHz. The maximum travel distance of the dither was around 100 nm. The QuIC photocurrent was detected at 2 kHz using a lock-in amplifier.

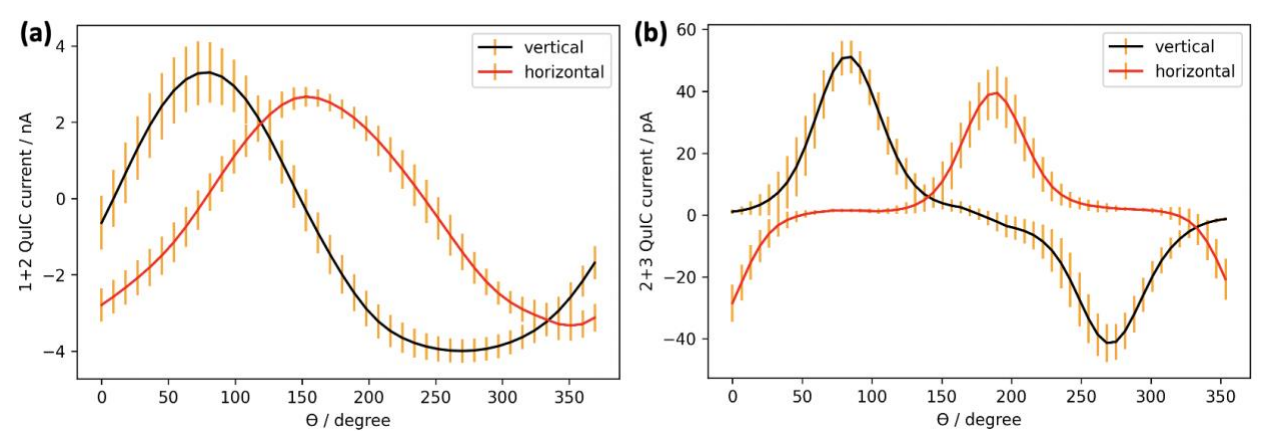


Figure 2: The polarization dependences of (a) 1+2 QuIC photocurrent and (b) 2+3 QuIC photocurrent from two excitation fields. Black line represents the photocurrent collected by the horizontal electrodes and red line represents the photocurrent collected by vertical electrodes.

The 2+3 QuIC photocurrent was measured with assistance of the offset frequency of the frequency comb, which was firstly measured using the heterodyne beat note produced in a 2f-to-3f self-referencing interferometer. Next, we controlled and stabilized the offset frequency of two frequency combs using a feed forward technique that compensated the fluctuations of the offset frequency at the -1 order diffracted beam of a AOM [2]. The offset frequencies of the 1040 nm beam and 1560 nm beam were set to be 14 kHz and 10 kHz respectively. The 1040 nm beam and 1560 nm beam were focused onto the center of four electrodes by a $60\times$ objective. The QuIC photocurrent was detected at 96 kHz using a lock-in technique.

For both 1+2 QuIC and 2+3 QuIC, two lock-in amplifiers were used to measure the injected photocurrents along k_x and k_y , respectively. In addition, each excitation beam passed through a half-wave plate (HWP). The reference frequencies of lock-in detection were set to be 2 kHz and 96 kHz for 1+2 QuIC and 2+3 QuIC respectively. The polarizations of two excitation beams in each experiment were kept coaligned and rotated together by HWPs. The angle between k_x and the polarization of excitation beams is denoted by Θ .

Figure 2 shows the polarization direction dependence of the QuIC photocurrent for 1+2 QuIC and 2+3 QuIC. The average and standard deviation of QuIC photocurrents were calculated with 50 rotation cycles of the polarizations. As shown by the black line in Figure 2 (a) and (b), the QuIC photocurrents collected by two horizontal electrodes peaked when two polarizations were along k_x . The maximum of photocurrent injected along k_x in 1+2 QuIC was ~2.2 nA. The maximum of photocurrent injected along k_x in 2+3 QuIC was ~38 pA. As shown by the red line in Figure 2 (a) and (b), the QuIC photocurrents collected by two vertical electrodes peaked when two polarizations were along k_y . The maximum of photocurrent injected along k_y in 1+2 QuIC was ~3.7 nA. The maximum of photocurrent injected along k_y in 2+3 QuIC was ~51 pA. The horizontal component of QuIC photocurrents maximized when the vertical component was near zero. In addition, the sign of QuIC photocurrents injected along an axis flipped when the projection of polarization on that axis flips sign. For both horizontal and vertical electrode pairs, the range of direction of polarization where 2+3 QuIC photocurrent vanishes is wider than that where 1+2 QuIC photocurrent vanishes. This shows that the distribution of injection carriers in k-space in 2+3 QuIC is more localized than that in 1+2 QuIC.

In summary, we measured the polarization direction dependence of the 1+2 QuIC current and the 2+3 QuIC current in AlGaAs collected by two pairs of orthognal ohmic electrodes. Our results indicate that the distribution of injected carriers in k-space in 2+3 QuIC is more localized than that in 1+2 QuIC, demonstrating a route to engineering the momentum-space distribution carriers generated by optical excitation.

References

[1] Peter A. Roos, Qudsia Quraishi, Steven T. Cundiff, Ravi D. R. Bhat, and J. E. Sipe, "Characterization of quantum interference control of injected currents in LT-GaAs for carrier-envelope phase measurements," Opt. Express 11, 2081-2090 (2003)

[2] Kai Wang, Rodrigo A. Muniz, J. E. Sipe, and S. T. Cundiff, "Quantum Interference Control of Photocurrents in Semiconductors by Nonlinear Optical Absorption Processes," Phys. Rev. Lett. 123, 067402

[3] Rodrigo A. Muniz, Cuauhtémoc Salazar, Kai Wang, S. T. Cundiff, and J. E. Sipe, "Quantum interference control of carriers and currents in zinc blende semiconductors based on nonlinear absorption processes" Phys. Rev. B 100, 075202 (2019)